

---

TRABAJO DE FIN DE GRADO

# NANOSTRUCTURES BASED ON AMPHIPHILIC JANUS DENDRIMERS AS DRUG CARRIERS AGAINST HEPATITIS C VIRUS

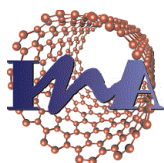
NANOESTRUCTURAS BASADAS EN DENDRÍMEROS  
JANO ANFIFÍLICOS COMO TRANSPORTADORES DE  
FÁRMACOS CONTRA EL VIRUS DE LA HEPATITIS C

**Julia Egido Egido**

Directores:

Olga Abián Franco  
José Luis Serrano Ostáriz

Universidad de Zaragoza, 2017



Instituto Universitario de Investigación  
en Nanociencia de Aragón  
Universidad Zaragoza



Instituto Universitario de Investigación  
Biocomputación y Física  
de Sistemas Complejos  
Universidad Zaragoza

# INDEX

1. Abstract / Resumen .....	1
2. Introduction .....	2
3. Objectives and work plan .....	5
4. Materials and methods .....	6
4.1. Synthesis and characterization .....	6
4.2. Formation of aggregates .....	9
4.3. Drug encapsulation .....	9
4.4. Dynamic light scattering .....	10
4.5. Transmission electron microscopy .....	10
4.6. Isothermal titration calorimetry .....	10
4.7. Cell cultures .....	11
4.8. Cell assays: viability and viral inhibition .....	12
5. Results and discussion .....	14
5.1. Synthesis of the bis-GMPA lipophilic dendron .....	14
5.2. Synthesis of the amphiphilic Janus dendrimer .....	15
5.3. Formation of dendritic aggregates and drug encapsulation .....	17
5.4. Study of the size and morphology of the nanoaggregates .....	18
5.5. Isothermal titration calorimetry .....	20
5.6. Cell viability and drug inhibition .....	21
6. Conclusions / Conclusiones .....	23
7. Bibliography .....	24
8. Annex .....	26



## 1 - ABSTRACT / RESUMEN

**ABSTRACT:** Despite improvements achieved in recent years, treatment of Hepatitis C still remains a challenge in some cases, posing the need to find new drugs against the HCV (Hepatitis C Virus). Some compounds which exhibit a high antiviral activity in primary screening do not succeed due to low activity *in vitro*, low solubility in water or high toxicity. Encapsulation of these compounds in nanocarriers could be a solution, and it may provide new therapeutic options against HCV. Among the different nanomaterials currently used as drug carriers, amphiphilic Janus dendrimers stand out due to their ability to form hydrosoluble aggregates with a lipophilic core. In this work, a new lipophilic dendron based on bis-GMPA has been synthesized. Using this dendron, an amphiphilic Janus dendrimer has been obtained by means of a “click chemistry” reaction. This dendrimer can form micellar aggregates with a high drug load capacity and so, it was tested as carrier for three drugs against HCV: camptothecin, tiratricol and iopanoic acid. Both the aggregates and the drug/carrier complexes have been characterized in several ways: morphology and size have been determined by transmission electron microscopy and dynamic light scattering, and the thermodynamics of the interaction between the different drugs and the dendrimer has been studied by isothermal titration calorimetry. Finally, the results of encapsulation on viral inhibition and cell viability have been assessed using an appropriate hepatic cell line culture. No conclusive results have been obtained regarding antiviral activity of the drug-loaded dendritic aggregates. However, the preliminary data obtained from this work suggest that this nanocarrier could improve the activity of the encapsulated drugs without affecting cell viability.

**RESUMEN:** A pesar de las mejoras conseguidas en los últimos años, el tratamiento de la Hepatitis C continúa siendo un reto en algunos casos, lo que plantea la necesidad de encontrar nuevos fármacos contra el VHC (Virus de la Hepatitis C). Ciertos compuestos que exhiben una alta actividad antiviral en *screenings* primarios no prosperan debido a baja efectividad *in vitro*, baja solubilidad en agua o alta toxicidad. Una posible solución es la encapsulación de estos compuestos en nanotransportadores, que podría proporcionar nuevas opciones terapéuticas contra el VHC. Entre los diferentes nanomateriales utilizados actualmente como transportadores de fármacos, los dendrímeros Jano anfífilicos destacan por su habilidad de formar agregados hidrosolubles con un núcleo lipídico. En este trabajo se ha sintetizado un nuevo dendrón lipófilo basado en bis-GMPA. A partir de este se ha obtenido un dendrímero Jano anfífilico mediante una reacción de “química click”. Este dendrímero puede formar agregados micelares con una alta capacidad de carga de fármaco, de modo que ha sido probado como transportador para tres fármacos contra el VHC: camptotecina, tiratricol y ácido iopanoico. Tanto los agregados como los complejos fármaco/dendrimer han sido caracterizados de varias maneras: la morfología y el tamaño se han determinado por microscopía de transmisión electrónica y dispersión dinámica de luz, y los parámetros termodinámicos de la interacción entre los diferentes fármacos y el dendrímero se ha estudiado por calorimetría isotérmica de titulación. Finalmente, se han evaluado los resultados de la encapsulación sobre la inhibición viral y la viabilidad celular, utilizando un cultivo de una línea celular hepática apropiada. No se han obtenido resultados concluyentes con respecto a la actividad antiviral de los complejos fármaco/dendrimer. Sin embargo, los datos preliminares obtenidos en este trabajo sugieren que este nanotransportador podría mejorar la actividad de los fármacos encapsulados sin afectar a la viabilidad celular.

## 2 - INTRODUCTION

In recent years, the development of new therapies has significantly improved the outlook of illnesses which used to be life-compromising. One of these is Hepatitis C. This disease is caused by the Hepatitis C virus (HCV), and can range in severity from an asymptomatic acute infection to a chronic disease. The latter is responsible in many cases for cirrhosis, hepatocellular carcinoma, and chronic kidney disease<sup>[1]</sup>. Nowadays, it is estimated that chronic HCV infection affects around 71 million people around the world, according to the World Health Organization<sup>[2]</sup>.

Hepatitis C virus (HCV) is a hepatotropic, enveloped, positive-sense single-stranded RNA virus of the Flaviviridae family. Its genome has an open reading frame and encodes a single polyprotein of approximately 3000 amino acids, which needs to be processed by at least two host cellular peptidases and two viral peptidases (NS2 and NS3/4A)<sup>[3]</sup>. The serin protease NS3/4A has been commonly used as a pharmacological target, along with NS5A (plays an important role in viral replication, assembly and cell signaling) and the RNA polymerase NS5B.

Current treatments for Hepatitis C are mainly based on combined therapies of what are called direct-acting antiviral agents (DAAs), for instance, the protease inhibitor simeprevir, the polymerase inhibitor sofosbuvir, or the NS5A inhibitors daclatasvir and ledispavir<sup>[4]</sup>. These are more specific than the previously used regimens, based on IFN- $\alpha$  and pegylated IFN- $\alpha$ , and can act against more than one viral genotype, succeeding to cure a high percentage of the cases while presenting a lower incidence of adverse events.

Nevertheless, approximately 400000 people die each year from Hepatitis C or complications associated to the chronic form of the disease<sup>[2]</sup>. For this reason, HCV infection is still a major health problem which needs to be addressed. The limitations of current treatments include the appearance of resistances and the low tolerability of certain drugs. This together with the limited access to diagnosis and treatment in certain places of the world where Hepatitis C is prevalent puts forth the need for an ongoing investigation aimed at the discovery of new therapeutic options.

In previous works carried out in our research group, several compounds with anti-HCV activity were identified: camptothecin, 3,3',5-triiodothyroacetic acid (tiratricol) and iopanoic acid. They are allosteric inhibitors of the HCV NS3 protease that bind to the Zn<sup>2+</sup>-free form of the enzyme, which is partially unfolded, stabilizing it<sup>[5]</sup>. In this way, they trap NS3 protease in its inactive conformational state. These compounds were identified by means of experimental ligand screenings<sup>[6][7]</sup>.

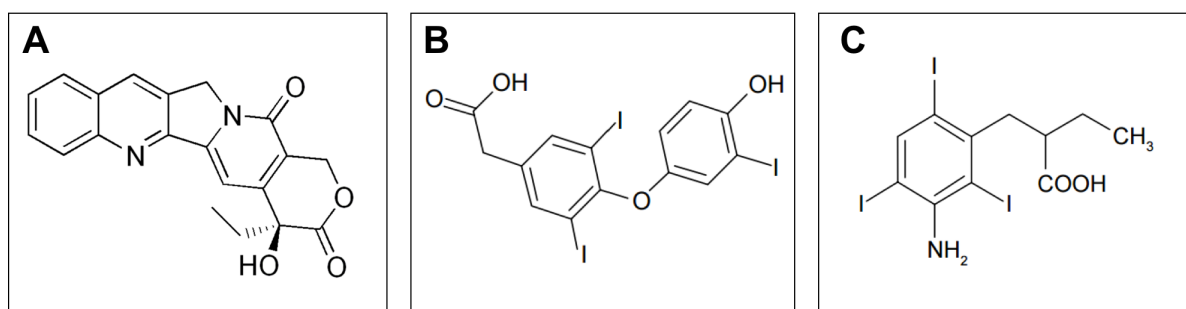


**Figure 1:** Skeletal formulas of camptothecin (A), tiratricol (B) and iopanoic acid (C).

Although these drugs are effective inhibitors of the NS3 protease, they exhibit several issues that needed to be improved. Camptothecin presents poor water solubility, low plasmatic stability and severe toxicity. Tiratricol and iopanoic acid have been seen to have low activity in cell assays (*in vitro*), which is thought to be due to hindered cell internalization. Consequently, these compounds would have initially been discarded as possible anti-HCV therapies.

Nevertheless, the pharmacokinetic properties of these compounds can be acted upon in order to solve the problems they present. It is here that nanomedicine plays a key role. The development of different kinds of nanomaterials as drug carriers has made it possible to increase the solubility and stability of the therapeutic compounds in the physiological medium, resulting in an enhanced bioavailability. This allows doses to be reduced, thus minimizing the risk of harmful side effects. Furthermore, *in vitro* bioactivity may be rescued since encapsulation in a nanocarrier can improve the access of an active principle to the infected cell. For instance, encapsulation of tiratricol and iopanoic acid in  $\gamma$ -cyclodextrins was seen to increase the anti-HCV activity of these compounds<sup>[7]</sup>.

Among the different nanomaterials used as platforms for drug delivery, dendrimers have gained a special interest over the past few decades. They are hyper-ramified polymers with a defined tree-like structure, made up of a certain number of repetitive units, depending on the generation and size of the dendrimer. They are practically monodisperse and present numerous peripheral groups that can be functionalized with different moieties. These characteristics make them more versatile and reproducible than other types of polymers<sup>[8]</sup>. The Liquid Crystals and Polymers Group, with which this project has been carried out, has specialized in the synthesis of different types of dendrimers for several applications, including drug and gene delivery.

In particular, platforms based on Janus dendrimers offer interesting features to this effect. Janus dendrimers, which receive their name from the two-faced Roman god Janus, are formed by two dendritic blocks (dendrons) that can have different terminal groups and hence different properties<sup>[9]</sup>. If one of the dendrons is lipophilic and the other is hydrophilic, the result is an amphiphilic molecule with the ability to self-assemble in aqueous solutions. This often results in micellar aggregates or bilayers whose morphology generally depends on the size proportion between the hydrophilic and lipophilic dendrons<sup>[10]</sup>.

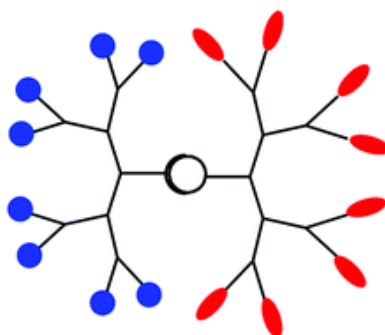


**Figure 2:** Schematic representation of a Janus dendrimer<sup>[9]</sup>.

A previous work was carried out in this group in which Janus dendrimers based on 2,2'-bis(hydroxymethyl)propionic acid (bis-MPA) dendritic blocks were used as camptothecin carriers<sup>[11]</sup>. The bis-MPA molecule offers several advantages: it can be synthesized in bulk

quantities, it has reactive groups that can be functionalized with organic and inorganic moieties, and the dendritic structures derived from it can be water soluble, biocompatible and hydrolytically degradable<sup>[12]</sup>. In this case, glycine moieties were added to the periphery of the hydrophilic dendron in order to enhance cellular internalization of the resulting ammonium-terminated aggregates.

Following this research line, a new type of hydrophilic poly(esteramide) dendrons was designed as part of the PhD thesis of Dr. Alexandre Lancelot<sup>[13]</sup>, carried out with the Liquid Crystals and Polymers group. These dendrons are based on 2,2'-bis(glycylmethyl)propionic acid (bis-GMPA), and contain both internal and peripheral glycine moieties. The dendrimers synthesized as a combination of bis-GMPA hydrophilic dendrons and bis-MPA lipophilic dendrons show a much higher efficiency in encapsulating camptothecin than that of the dendrimers only based in bis-MPA. This can be explained by the potential formation of hydrogen bonds between the lactone, hydroxyl and ketone groups of the drug and the internal amide groups of the dendron.

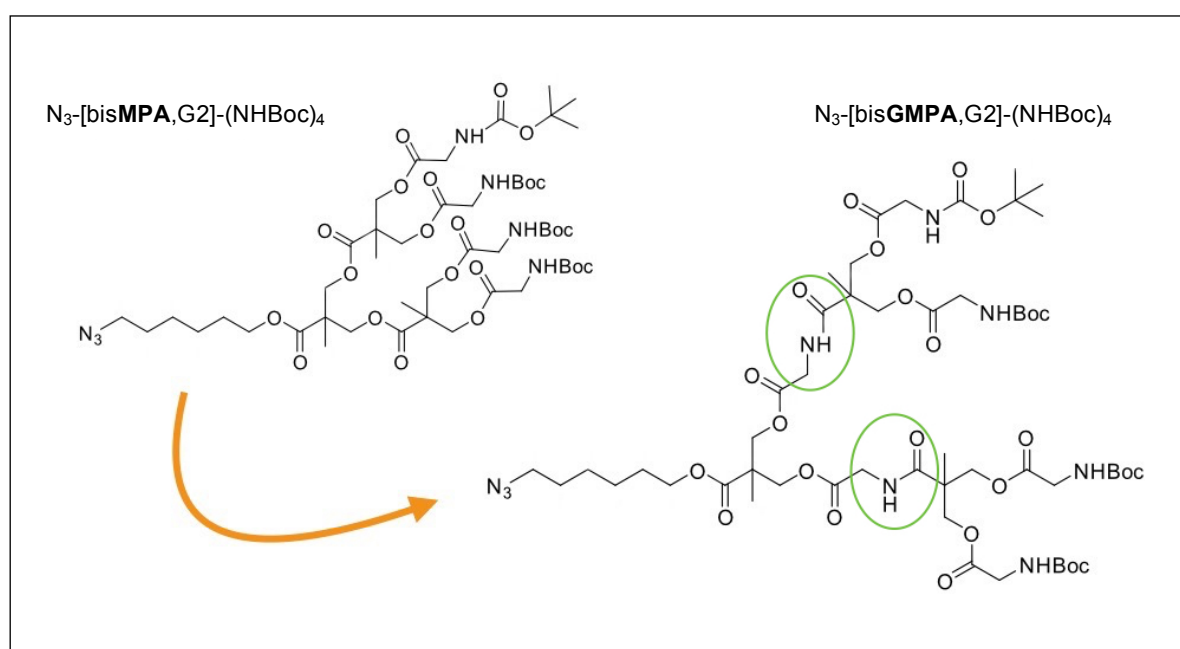


**Figure 3:** Comparison between the structures of hydrophilic dendrons of generation 2 based on bis-MPA ( $N_3$ -[bisMPA,G2]-(NHBoc)<sub>4</sub>) and bis-GMPA ( $N_3$ -[bisGMPA,G2]-(NHBoc)<sub>4</sub>). The internal glycine moieties introduced in the bis-GMPA dendrons are circled in green.

However, the resulting dendrimer/camptothecin conjugates fail to improve the cell viability and HCV inhibitory activity values obtained for free camptothecin. A reason for this may be the location of the drug in these aggregates. Since the glycine residues with which it interacts are part of the hydrophilic, more polar dendron, the drug is possibly located in a partially hydrophilic environment that could promote the hydrolysis of its lactone ring, which occurs at physiological pH.

### 3 - OBJECTIVES AND WORK PLAN

Taking into account the antecedents described in the Introduction, two main **objectives** for this work were proposed:

1. **The synthesis and characterization of a new kind of amphiphilic Janus dendrimer based on a bis-MPA hydrophilic dendron and a bis-GMPA lipophilic dendron.** This design aims to solve the limitations of the aforementioned dendrimers, by inserting the stabilizing glycine moieties in a more lipophilic environment which may better preserve the activity of the drugs.
2. **The study of the transport properties of the aggregates formed with this new dendrimer as carriers of the three compounds previously described (camptothecin, tiratricol and iopanoic acid),** so as to assess their effectiveness in reducing drug cytotoxicity and maintaining or enhancing the *in vitro* antiviral activity of these compounds.

In order to reach these objectives we followed this sequential **work plan**:

- Synthesis and characterization of a new lipophilic dendron based on bis-GMPA.
- Synthesis and characterization of an amphiphilic Janus dendrimer formed by the bis-GMPA lipophilic dendron and a bis-MPA hydrophilic dendron functionalized with ammonium terminal groups.
- Determination of the ability to self-assemble in water of the dendrimer and characterization of the size and morphology of the resulting nanoaggregates.
- Encapsulation of camptothecin, tiratricol and iopanoic acid in the nanoaggregates:
  - Quantification of the amount of drug encapsulated and determination of the encapsulation efficiencies.
  - Study of the interaction between the drugs and the dendrimer.
  - Characterization of the size and morphology of the dendrimer/drug conjugates.
- *In vitro* determination of the effects on viral replication and cell viability of the dendritic nanoaggregates and the dendrimer/drug conjugates.



## 4 - MATERIALS AND METHODS

### 4.1 - Synthesis and characterization

Solvents were purchased from Scharlab, S.L. All reagents and camptothecin, were purchased from Sigma-Aldrich or Acros and were used without further purification. TBTA (tris(benzyltriazolylmethyl)amine), saturated solution of HCl in ethyl acetate, DPTS (4-(dimethylamino)pyridium 4-toluenesulfonate) and bis-MPA monomer were prepared in our laboratory.

$^1\text{H}$  NMR and  $^{13}\text{C}$  NMR experiments were performed using a Bruker AV-400 ( $^1\text{H}$ : 400 MHz,  $^{13}\text{C}$ : 100 MHz) spectrometer. The chemical shifts are given in ppm relative to TMS (tetramethyl silane) and the coupling constants in Hz; the solvent residual peak was used as internal standard. Mass spectrometry (MS) was performed on a Bruker Microflex system employing the ESI or the MALDI-TOF technique with nitrogen laser (337 nm) and dithranol as matrix. Infrared spectra were obtained on a Bruker Vertex 70 spectrophotometer in ATR (attenuated total reflection) mode. Gel permeation chromatography was performed on a Waters e2695 Alliance system with two Styragel columns HR4 and HR1 (500 and  $10^4$  Å of pore size) in series and a Waters 2424 evaporation light scattering detector with a sample concentration of 1 mg/mL. The solvent used was tetrahydrofuran (HPLC grade) with a flow rate of 1 mL/min at 35° C; PMMA (poly(methyl methacrylate) was used as the standard for calibration. Elemental Analysis (EA) was performed with a Perkin-Elmer 2400 series II microanalyser.

Synthesis and characterization of the lipophilic dendron ( $\equiv$ -[bisGMPA,G1]-(C17) $_2$ ): functionalization of the dendron with stearic acid (C17 alkyl chains)

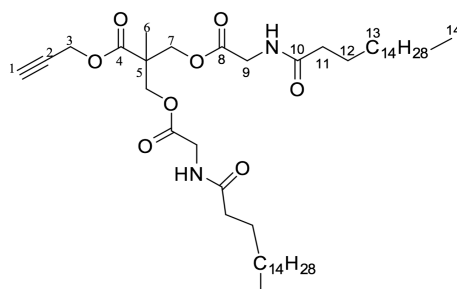


**Figure 4:** Skeletal structure of  $\equiv$ -[bisGMPA,G1]-(C17) $_2$ .

Stearic acid (2.37 g, 8.34 mmol, 3 eq.), 4-(dimethylamino) pyridine (DMAP) (0.27 g, 2.22 mmol, 0.8 eq.) and 1-hydroxybenzotriazole (HOBt) (1.28 g, 8.34 mmol, 3 eq.) were dissolved into anhydrous dichloromethane (86 mL). The reaction mixture was stirred under argon atmosphere. Dicyclohexylcarbodiimide (DCC) (1.72 g, 8.34 mmol, 3 eq.) was dissolved into a minimal volume of anhydrous dichloromethane (4 mL) and added dropwise to the reaction mixture.  $\equiv$ -[bisGMPA,G1]-(NH $_3^+$ Cl) $_2$  (1 g, 2.78 mmol, 1 eq.; described in the Annex, pages 36-38) was dissolved into 10 mL of anhydrous dimethyl sulfoxide, together with DMAP (0.68 g, 5.56 mmol, 2 eq.). This mixture was then added dropwise to the aforementioned reaction mixture with a dropping funnel. The final reaction mixture was stirred at room temperature under argon atmosphere during 48 hours. A white precipitate appeared ( $N,N'$ -

dicyclohexylurea), which was filtered off. The solvent was then evaporated under vacuum. The crude product was dissolved into a minimal volume of dichloromethane and purified by precipitation into cold acetone overnight. The precipitate was further purified through silica gel column chromatography (dichloromethane : methanol = 98 : 2). A brown solid was obtained (1856 mg, yield = 81.5%).

**Mw** = 819.21 g/mol.

**<sup>1</sup>H NMR** (400 MHz, CDCl<sub>3</sub>) δ (ppm): 6.16 (bs, 2H, -NH), 4.72 (d, *J* = 2.4 Hz, 2H, H-3), 4.32 (m, 4H, H-7), 4.01 (d, *J* = 5.4 Hz, 4H, H-9), 2.50 (t, *J* = 2.4 Hz, 1H, H-1), 2.27 – 2.19 (m, 4H, H-11), 1.68 – 1.57 (m, 4H, H-12), 1.28 (s, 3H, H-6), 1.24 (d, *J* = 14.9 Hz, 56H, H-13), 0.87 (t, *J* = 6.8 Hz, 6H, H-14).

**<sup>13</sup>C NMR** (100 MHz, CDCl<sub>3</sub>) δ (ppm): 173.69 (C-10), 171.80 (C-4), 169.76 (C-8), 75.57 (C-1), 65.76 (C-7), 52.91 (C-3), 46.33 (C-5), 41.23 (C-9), 36.47 (C-11), 32.06 (C-13), 29.94 – 29.33 (C-13'), 25.68 (C-12), 22.82 (C-13''), 18.15 (C-6), 14.25 (C-14).

**FTIR** (*v*<sub>max</sub>/cm<sup>-1</sup>, ATR): 3294 (N-H st), 2955 and 2916 (C-H st), 1744 (C=O ester st), 1645 (C=O amide st), 1555 (N-H δ), 1470 (CH<sub>2</sub>, CH<sub>3</sub> δ), 1203 (C-O st).

**MS** (ESI<sup>+</sup>) *m/z* (%): found 841.5 (100), calculated for [C<sub>48</sub>H<sub>86</sub>N<sub>2</sub>O<sub>8</sub>,Na]<sup>+</sup> 841.63.

**EA** (%): Found: C, 70.12; H, 10.45; N, 3.34. Calc. for C<sub>48</sub>H<sub>86</sub>N<sub>2</sub>O<sub>8</sub>: C, 70.37; H, 10.58; N, 3.42.

**GPC**: (ref PMMA): Mw 2340 g.mol<sup>-1</sup>; Đ 1.04.

Synthesis and characterization of the protected dendrimer ((NHBoc)<sub>8</sub>[bisMPA,G3]-[bisGMPA,G1](C17)<sub>2</sub>): copper(I) azide-alkyne cyloaddition reaction (CuAAC)

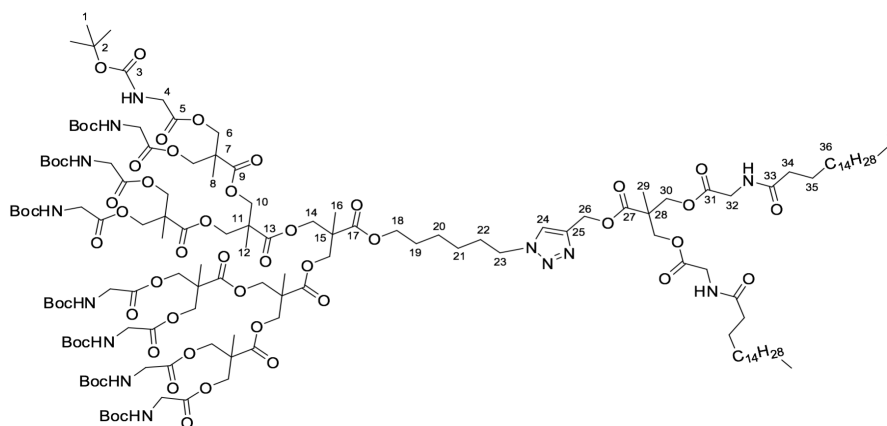


**Figure 5:** Skeletal structure of ((NHBoc)<sub>8</sub>[bisMPA,G3]-[bisGMPA,G1](C17)<sub>2</sub>).

Hydrophilic bis-MPA dendron of generation 3 (900 mg, 407 μmol, 1 eq.) and ≡-[bisGMPA,G1]-(C17)<sub>2</sub> (400 mg, 488 μmol, 1.2 eq.) were dissolved into dimethylformamide (DMF; 7 mL) in a Schlenk flask. The reaction mixture (azide-alkyne reaction mixture) was subjected to 3 vacuum-argon cycles in order to remove the O<sub>2</sub> and stirred under argon atmosphere at 45°C. CuSO<sub>4</sub>·5H<sub>2</sub>O (11.99 mg, 40.7 μmol, 0.1 eq.), L-ascorbate (16.13 mg, 81.4 μmol, 0.2 eq.) and TBTA (27.58 mg, 40.7 μmol, 0.1 eq.) were dissolved into DMF (3 mL) in a second Schlenk flask. This solution also underwent 3 vacuum-argon cycles and was

then stirred at 45° C during 15 min. Next, it was added through a cannula to the azide-alkyne reaction mixture. The resulting reaction mixture was stirred at 45° C during 2 days. After this, a mixture of brine (50 mL) and water (50 mL) was added and the product was extracted twice with ethyl acetate (2 x 70 mL). The organic phase was washed three times with a mixture of brine (75 mL) and water brine (25 mL), once with a KCN aqueous solution (15 mg into 100 mL of water) and twice with brine (2 x 100 mL) and dried over anhydrous MgSO<sub>4</sub>. The solvent was removed under reduced pressure and the crude product purified through silica gel column chromatography (dichloromethane : methanol = ramp from 100:0 to 96:4). The product was further purified by dialysis (MWCO = 1000 Da) in methanol during 24 hours, to obtain a white powder (334 mg; yield = 27%).

**Mw** = 3032.54 g/mol.

**<sup>1</sup>H NMR** (400 MHz, CDCl<sub>3</sub>) δ (ppm): 7.74 (s, 1H, H-24), 6.43 (bs, -NHCO), 5.38 (bs, -NHBOc), 5.25 (s, 2H, H-26), 4.39 (t, *J* = 6 Hz, 2H, H-23), 4.26 (m, 32H, H-6, H-10, H-14 and H-30), 4.20 (t, *J* = 6 Hz, 2H, H-18), 3.88 (s, 20H, H-4 and H-32), 2.24 (t, *J* = 8 Hz, 4H, H-34), 1.80 (t, *J* = 5 Hz, 2H, H-22), 1.44 (s, 72H, H-1), 1.28 (s, 12H, H-8), 1.25 (s, 40H, H-12, H-16, H-29 and H-36), 0.88 (t, *J* = 6.8 Hz, 6H, H-37).

**<sup>13</sup>C NMR** (100 MHz, CDCl<sub>3</sub>) δ (ppm): 173.89 (C-9), 172.43 (C-13), 172.17 (C-17), 172.00 (C-27), 171.69 (C-33), 170.23 (C-31), 169.73 (C-5), 156.04 (C-3), 80.06 (C-2), 65.83 (C-10, C-14, C-18 and C-30), 65.5 (C-6), 46.53 (C-7, C-11, C-15 and C-28), 42.36 (C-32), 41.19 (C-4), 36.41 (C-34), 32.04 (C-22), 29.82 (C-19 and C-35), 29.65 (C-12, C-16 and C-29), 28.45 (C-1), 25.70 (C-21), 22.80 (C-20), 18.05 (C-36), 17.68 (C-8), 14.24 (C-37).

**FTIR** (*v*<sub>max</sub>/cm<sup>-1</sup>, ATR): 3370 (N-H st), 2922 and 2852 (C-H st), 1742 (C=O st ester), 1718 (C=O st carbamate), 1522 (N-H δ), 1470 (CH<sub>2</sub>, CH<sub>3</sub> δ), 1367 (C-N st), 1157 (N-CO-O st).

**MS** (ESI<sup>+</sup>) *m/z* (%): found 3055.8 (100), calculated for [C<sub>145</sub>H<sub>243</sub>N<sub>13</sub>O<sub>54</sub>,Na]<sup>+</sup> 3053.66.

**EA** (%): Found: C, 57.15; H, 8.94; N, 5.78. Calc. for C<sub>145</sub>H<sub>243</sub>N<sub>13</sub>O<sub>54</sub>: C, 57.43; H, 8.08; N, 6.00.

**GPC**: (ref PMMA): Mw 6346 g.mol<sup>-1</sup>; Đ 1.05.

Synthesis and characterization of the deprotected dendrimer ((NH<sub>3</sub><sup>+</sup>Cl)<sub>8</sub>[bisMPA,G3]-[bisGMPA,G1](C17)<sub>2</sub>): deprotection of the amino terminal groups

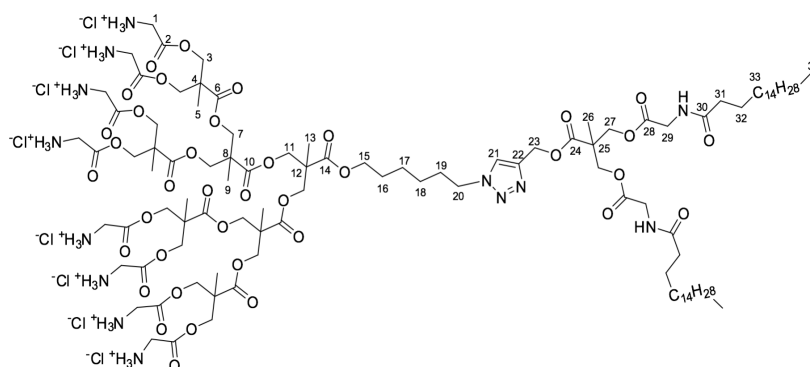


**Figure 6:** Skeletal structure of (NH<sub>3</sub><sup>+</sup>Cl)<sub>8</sub>[bis-MPA,G3]-[bis-GMPA,G1](C17)<sub>2</sub>.

(NHBoc)<sub>8</sub>[bisMPA,G3]-[bisGMPA,G1](C17)<sub>2</sub> (280 mg, 92.33 μmol) was dissolved into ethyl acetate (2 mL). Hydrochloric acid into ethyl acetate (3M, 6 mL) was added to it. The reaction mixture was stirred at room temperature during 45 minutes until a white precipitate appeared. It was then diluted into ethyl acetate and stirred during another 30 minutes. The hydrochloric acid was removed under vacuum. The reaction mixture was centrifuged and the precipitate was recovered and washed twice with pure ethyl acetate. The product was finally obtained as a white powder (220 mg, yield = 94%).

**Mw** = 2523.30 g/mol.

**<sup>1</sup>H NMR** (400 MHz, MeOD) δ (ppm): 8.10 (s, 1H, H-21), 5.27 (s, 2H, H-23), 4.50 – 4.39 (m, 18H, H-3 and H-20), 4.40 – 4.22 (m, 16H, H-7, H-11 and H-27), 4.15 (t, *J* = 6.0 Hz, 2H, H-15), 3.96 (s, 16H, H-1), 3.88 (s, 4H, H-29), 2.26 (t, *J* = 7.0 Hz, 4H, H-31), 1.95 (m, 2H, H-19), 1.69 (m, 2H, H-16), 1.62 (m, 4H, H-32), 1.45 (m, 4H, H-17 and H-18), 1.33 (s, 12H, H-5), 1.29 (m, 65H, H-9, H-13 and H-33), 1.25 (s, 3H, H-26), 0.90 (t, *J* = 6.6 Hz, 6H, H-34).

**<sup>13</sup>C NMR** (100 MHz, MeOD) δ (ppm): 176.79 (C-6), 173.93 (C-10), 173.75 (C-14), 173.37 (C-24), 173.23 (C-30), 170.84 (C-28), 168.39 (C-2), 143.57 (C-22), 126.22 (C-21), 67.58 (C-7, C-11, C-15 and C-27), 66.82 (C-3), 59.05 (C-23), 51.34 (C-20), 47.60 (C-4, C-8, C-12 and C-25), 41.92 (C-29), 41.15 (C-1), 36.78 (C-31), 33.05 (C-19), 31.12 (C-16 and C-32), 30.87 – 30.07 (C-9, C-13 and C-26), 26.95 (C-18), 26.44 (C-17), 23.71 (C-33), 18.17 (C-5), 14.45 (C-34).

**FTIR** (*v*<sub>max</sub>/cm<sup>-1</sup>, ATR): 3674-3202 (N-H st), 3202-2600 (N-H<sup>+</sup> st), 2962-2920-2851 (C-H st), 1734 (C=O st ester), 1647 (C=O amide st), 1472 (CH<sub>2</sub>, CH<sub>3</sub> δ), 1217 (C-O st), 1128 (O-C-C st).

**MS** (ESI<sup>+</sup>) *m/z* (%): found 2254.0 (100), calculated for [C<sub>105</sub>H<sub>179</sub>N<sub>13</sub>O<sub>38</sub>,Na]<sup>+</sup> 2253.24.

**EA** (%): *Found*: C, 48.54; H, 8.35; N, 6.8. *Calc. for* C<sub>105</sub>H<sub>187</sub>N<sub>13</sub>O<sub>38</sub>Cl<sub>8</sub>: C, 49.98; H, 7.47; N, 7.22.

## 4.2 - Formation of aggregates

The formation of aggregates of the amphiphilic dendrimer was carried out by the oil-in-water method<sup>[14]</sup>. The dendrimer was dissolved at a concentration of 1 mg/mL in dichloromethane. An identical volume of distilled water to that of dichloromethane was added. The mixture was stirred at room temperature with an IKA KS 130 basic orbital shaker until the organic solvent, which is highly volatile and water-immiscible, had completely evaporated. The final concentration of the dendrimer in water was 1 mg/mL.

## 4.3 - Drug encapsulation

Encapsulation of camptothecin, tiratricol and iopanoic acid inside the aggregates was carried out by means of the solvent diffusion technique<sup>[15]</sup>. In the case of camptothecin, a solution of the drug into DMSO (200 μg/mL) was added to the previously prepared aggregates (in aqueous medium), so that the final solution contained 100 μg of camptothecin per mg of dendrimer. In the case of tiratricol and iopanoic acid, a solution of the drug into DMSO (1 mg/mL) was added to the aggregates, so that the final solution contained 500 μg of the drug per mg of dendrimer. In all cases the volume of DMSO added was equal to half the volume of water. The mixtures were stirred at 4° C for 12 h, allowing the drug to reach the lipophilic core of the aggregates. DMSO was removed by dialysis against distilled water at 4° C using

a 1000 Da membrane. The non-encapsulated drugs (especially camptothecin) precipitated during the dialysis and were removed by filtration to obtain the dendrimer/CPT aggregates.

The concentration of encapsulated camptothecin was measured by fluorescence ( $\lambda_{\text{max}} = 436$  nm and  $\lambda_{\text{exc}} = 368$  nm). 100  $\mu\text{L}$  of the filtered solution were dissolved into 1900  $\mu\text{L}$  of DMSO in order to break the aggregates and ensure drug release. The intensity of the fluorescence maximum was compared to a calibration curve ranging from 0 ng/mL to 50 ng/mL. The concentration of encapsulated tiratricol and iopanoic acid was measured by UV-Vis absorbance (tiratricol  $\lambda_{\text{max}} = 300$  nm; iopanoic acid  $\lambda_{\text{max}} = 317$  nm). The samples were diluted into DMSO (1:3) in order to break the aggregates and ensure drug release, without allowing DMSO absorbance to affect the measurements. The intensities of the absorbance maxima were compared to a calibration curve ranging from 0  $\mu\text{g/mL}$  to 170  $\mu\text{g/mL}$ . The fluorescence emission spectra were obtained on a Perkin-Elmer-Ls 55 system. The UV-Vis absorbance spectra of the samples were measured with a Varian Cary 50 probe UV-Vis spectrophotometer. The calibration curves for the three compounds can be found in the Annex (figure A33).

#### **4.4 - Dynamic light scattering (DLS)**

This technique that allows to determine the size distribution profile of particles in a solution. It generates data by measuring the light scattering produced when a laser beam hits spherical particles.

The nanoaggregates both empty and encapsulating the drugs were studied with a Malvern Instruments Nano ZS that uses a He-Ne laser with a wavelength of 633 nm and a detection angle of 173°.

#### **4.5 - Transmission electron microscopy (TEM)**

TEM images and measurements were obtained using the bright field operation mode. The samples were prepared by depositing a drop of an aqueous solution containing the dendrimeric aggregates or the dendrimer/drug conjugates on a holey carbon film 300 Mesh Cu (50) grid from Agar Scientific. The liquid was removed and the sample was stained with an aqueous solution of phosphotungstic acid (3%). After the liquid was removed, the samples were allowed to dry for at least 24 hours.

The TEM experiment was performed in a TECNAI G20 (FEI COMPANY), 200 kV, at the Laboratory of Advanced Microscopy (LMA) of the INA (Nanosciences Institute of Aragon).

Width value for each drug/carrier conjugate was calculated as the mean of the widths of 50 different micelles measured on 5 different images.

#### **4.6 - Isothermal titration calorimetry (ITC)**

This technique that studies the thermodynamic interactions between two molecules, allowing to determine directly  $K_a$ ,  $\Delta H$  and  $N$  of the interaction. The apparatus consists of two cells (sample cell and reference cell) and a syringe that injects aliquots of a ligand sequentially into the sample cell, which are then stirred. What is measured is the thermal power needed to maintain the reference cell and the sample cell at an identical temperature against time<sup>[16]</sup>. The reference cell contains water or buffer solution, while the sample cell contains a

molecule which, upon interaction with the ligand, releases or absorbs heat. In this case, the equipment in which the measurements were carried out was an Auto-iTC200 Isothermal Titration Calorimetry (MicroCal, GE Healthcare).

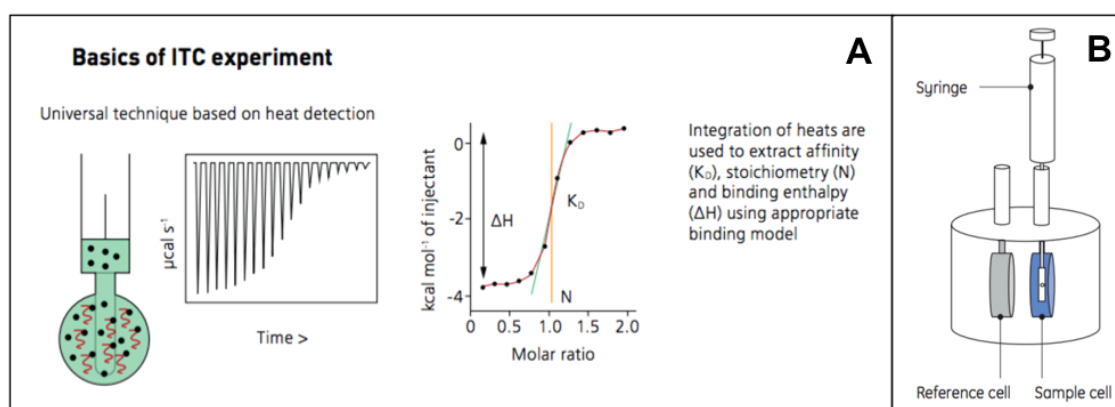


**Figure 7:** Schematic drawing of the basic functioning of an ITC experiment (**A**) and an ITC equipment (**B**). Images taken from the apparatus's commercial brochure (Malvern).

The syringe was fed 150  $\mu\text{L}$  of the drug solution (final concentration = 100  $\mu\text{M}$ ). The sample cell was fed 400  $\mu\text{L}$  of a solution containing the dendrimer (final concentration = 10  $\mu\text{M}$ ). A pre-rinse solution was also prepared containing the same composition as that used for the sample cell except for the molecules involved in the interaction.

Data management, integrations and curve fitting were performed using Origin 7.0.

	Cell	Syringe	Pre-rinse
Milli-Q water	386 $\mu\text{L}$	148.5 $\mu\text{L}$	396 $\mu\text{L}$
DMSO	4 $\mu\text{L}$	-	4 $\mu\text{L}$
Drug (10 mM in DMSO)	-	1.5 $\mu\text{L}$	-
Dendrimer (400 $\mu\text{M}$ in water)	10 $\mu\text{L}$	-	-

**Table 1:** Concentrations and volumes used for the ITC experiments.

## 4.7 - Cell cultures

The cell studies carried out in this work were performed on cells of the Huh 5-2 line. They are obtained by transfecting the subgenomic HCV replicon *1389luc-ubi-neo/NS3-3'/5.1* into the highly permissive cell clone Huh 7-Lunet, established from a hepatocellular carcinoma<sup>[17]</sup>.

The replicon system mimics the viral replication cycle, and allows to assess the effects of drugs on viral replication while minimizing the risks of working with viable viral particles. It contains the sequence encoding HCV non-structural proteins that are essential for replication (coding region from NS3 to 3'-NTR), along with a selection system consisting of a reporter gene, *Photinus pyralis* luciferase, and the antibiotic resistance marker neomycin phosphotransferase, which confers resistance to geneticin (G418). The genetic construction also contains the 5'-NTR region of the encephalomyocarditis virus (ECMV) and an internal ribosome entry site<sup>[18]</sup>.

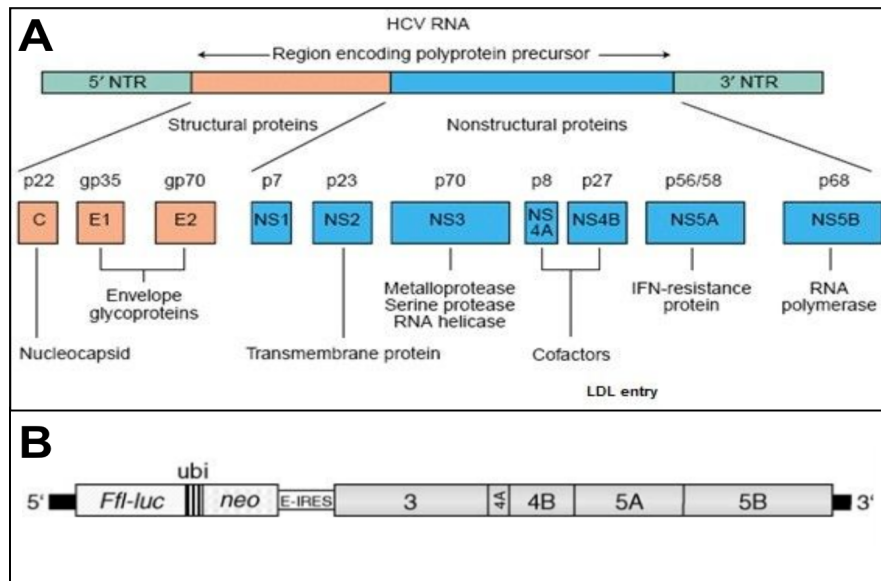


**Figure 8:** Genome of the HCV: regions and proteins coded<sup>[19]</sup> (A); genetic construct of the replicon system contained in Huh 5-2 cells<sup>[20]</sup> (B).

Cells were grown in Dulbecco's Modified Eagle's Medium (DMEM) with or without phenol red, supplemented with 10% heat-inactivated fetal bovine serum, 100 IU/mL penicillin, 100 µg/mL streptomycin, and 250 µg/mL geneticin (G418), under conditions of constant temperature (37° C), pressure (1 atm) and CO<sub>2</sub> concentration (5% CO<sub>2</sub>, 95% air).

Since Huh 5-2 cells are adherent, incubation with trypsin-EDTA 0.05% (5-10 minutes at 37° C) was necessary prior to subcultivations. PBS was used to eliminate cell residues. All cell culture media and reagents used were pre-warmed at 37° C so as not to affect cell metabolism, and all manipulations were carried out in a laminar flow hood, respecting all due precautions in order to avoid contaminations.

DMEM (Dulbecco's modified Eagle's medium, 4.5 g/L glucose), DPBS (Dulbecco's phosphate-buffered saline) and geneticin (G418) were purchased from Gibco. Penicillin/41 streptomycin (5000 U/mL) and trypsin-Versene (EDTA) were purchased from Lonza. Fetal bovine serum was purchased from PAN-Biotech GmbH.

#### 4.8 - Cell assays: viability and viral inhibition

For these assays cells were seeded at a density of 7000 cells per well in the complete DMEM medium without phenol red in a 96-well plate (white plates in the case of the viral inhibition assay and transparent plates in the case of the cell viability assay). Cell concentration was determined using a Scepter™ 2.0 Cell Counter (Millipore). They were allowed to grow for 24 hours. After this the medium was removed.

Solutions containing different concentrations of the drugs, dendrimer/drug conjugates or the dendrimer aggregates and 2% DMSO in complete DMEM medium without phenol red were prepared. Triplicates of each concentration were made by adding 100 µL per well of the different solutions. The cells were then incubated for 72 hours prior to the realization of the

assays. A scheme representing the setup of the plates can be found in the annex (figure A34).

To assess the cytotoxicity of both the drugs and the dendrimer, cell metabolism levels were determined using Promega's Cell Titer 96® AQueous kit. It is a colorimetric method based on the conversion of MTS (3-(4,5-dimethylthiazol-2-yl)-5-(3-carboxymethoxyphenyl)-2-(4-sulfophenyl)-2H-tetrazolium salt) into formazan, which only occurs in living cells, due to the activity of the succinate-tetrazolium reductase (Technical Bulletin CellTiter 96® AQueous One Solution Cell Proliferation Assay). For this assay, 20 µL of the CellTiter 96® AQueous One Solution Reagent were added to each well, and the plates were incubated for an hour and a half in the conditions described in the previous section. Absorbance of the formazan products was then measured at 490 nm in a Synergy™ HTX Multi-Mode Microplate Reader. Absorbance at 800 nm (non-specific) was also measured and subtracted from the absorbance at 490 nm (specific). Data were obtained using the Gen5™ Data Analysis software. The 50% cytotoxic concentration (CC50) was calculated as the drug concentration that reduced cell viability by 50% compared to untreated controls.

The antiviral activity of the different compounds was determined using Promega's Bright-Glo™ Luciferase Assay System kit. This kit allows to indirectly measure the replication rate of the HCV replicon system of the Huh 5-2 cells. These cells express luciferase and neomycin phosphotransferase as a fusion protein. If the viral serin-protease NS3 is expressed, luciferase is released and free to oxidize its specific substrate, luciferin (present in the Bright-Glo™ Luciferase Assay Substrate). This reaction is carried out in the presence of Mg<sup>2+</sup>, ATP and O<sub>2</sub>, and yields oxyluciferin, which is fluorescent. The formation of this product results in a luminiscence signal that is proportional to the quantity of RNA from the replicon system that is being expressed (Technical Manual Bright-Glo™ Luciferase Assay System). For this assay, 20 µL of the Bright-Glo™ Luciferase Assay Substrate were added to each well, and the plates were incubated for an hour and a half in the conditions described in the previous section. Luminiscence was measured in a Synergy™ HTX Multi-Mode Microplate Reader. Data were obtained using the Gen5™ Data Analysis software. The 50% inhibitory concentration (CC50) was calculated as the drug concentration that inhibited viral replication by 50% compared to untreated controls.



## 5 - RESULTS AND DISCUSSION

### 5.1 - Synthesis of the bis-GMPA lipophilic dendron

A new lipophilic bis-GMPA dendron bearing an alkyne group at its focal point and two terminal aliphatic linear chains of seventeen carbons (C17) was synthesized. The pathway followed is represented in the next scheme (all of the molecules except the precursors were synthesized as part of this work; the synthetic procedures and results of their characterization can be found in the Annex):

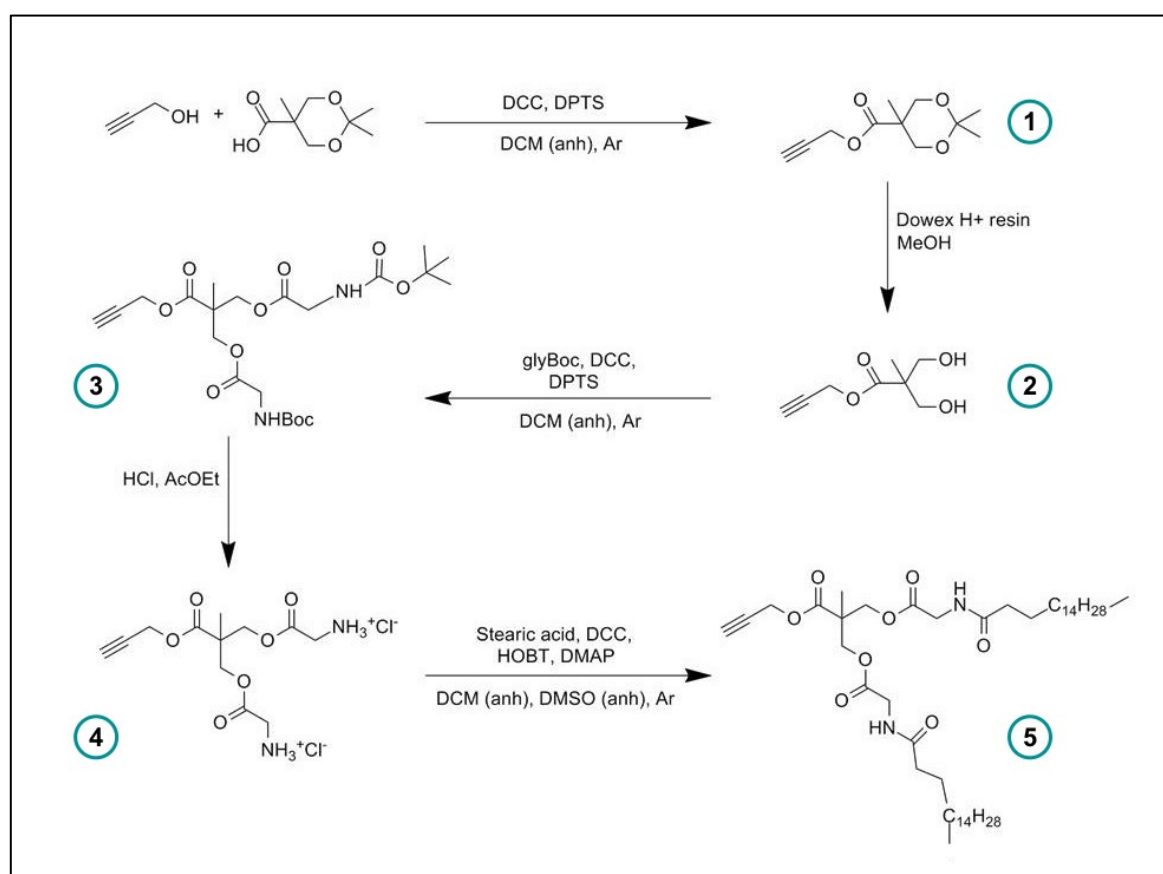


**Figure 9:** Synthesis scheme of reactions leading to the bis-GMPA lipophilic dendron (molecule 5).

The propargyl group was inserted at the focal point of the acetal-protected bis-MPA monomer by means of a Steglich esterification (molecule 1). Following reductive deprotection (molecule 2), the same kind of reaction was carried out in order to introduce the internal glycine moieties (molecule 3). After the amino-terminal groups were deprotected (molecule 4), the dendron was functionalized with the aliphatic chains by means of an amidation between the amino-terminal groups and stearic acid, again following conditions similar to those of a Steglich reaction.

In general, the Steglich esterifications were carried out under Argon atmosphere using anhydrous dichloromethane as solvent. In this kind of reaction, DCC (dicyclohexylcarbodiimide) acts as a coupling agent and is transformed into DCU (dicyclohexylcarbodiurea), which needs to be removed by precipitation in hexane and

filtration. DPTS (4-(dimethylamino)pyridium 4-toluenesulfonate) acts as a catalyst and is regenerated after the esterification. The crude products must be purified by flash chromatography on silica gel.

In the case of the reaction yielding the final dendron (molecule 5), some modifications of this protocol were made: HOBt (hydroxybenzotriazole) was also used as a coupling agent, and DPTS was substituted by DMAP (4-(dimethylamino)pyridine). This reagent neutralizes the acidic ammonium salts of the dendrons, favoring the amidation. In addition, anhydrous DMSO (dimethyl sulfoxide) was employed to dissolve the precursor compound (4).

Each of the molecules was characterized by  $^1\text{H}$  and  $^{13}\text{C}$  nuclear magnetic resonance (NMR), mass spectrometry (MS), Fourier transform infrared spectroscopy (FTIR) and elemental analysis (EA), in order to assess their integrity and purity.

In particular, the following  $^1\text{H}$  NMR results confirmed that the synthesis and functionalization of the final dendron had been successful:

- The appearance of four peaks at 0.87, 1.24, 1.63 and 2.23 ppm, corresponding respectively to the terminal methyl proton (0.87 ppm) and to the methylene protons (rest of the peaks) of the aliphatic chain indicated the incorporation of the stearic acid.
- The shift of the peak corresponding to the N-H proton from 8.56 ppm (in the  $^1\text{H}$  NMR spectrum obtained for molecule 4) to 6.16 (in the  $^1\text{H}$  NMR spectrum obtained for molecule 5) further confirmed that amidation between the amino-terminal groups present in molecule 4 and the stearic acid had taken place.
- In addition, peaks corresponding to the protons of the propargyl moiety (a triplet at around 2.50 ppm and a doublet at around 4.72 ppm) could be observed in the spectra of all the molecules (1-5).

## 5.2 - Synthesis of the amphiphilic Janus dendrimer

The synthesis of the dendrimer was carried out by linking the lipophilic dendron with a bis-MPA hydrophilic dendron (molecule 6), previously synthesized by Dr Alexandre Lancelot as part of the work of his PhD thesis<sup>[13]</sup>.

This was achieved by means of a copper(I)-catalyzed azide-alkyne cycloaddition (CuAAC) through which the alkyne group of the lipophilic dendron and the azide group of the hydrophilic dendron are joined to form a triazole ring. This can be considered a “click chemistry” reaction.

The Cu(I) catalyst was formed in situ by reduction of the copper (II) salt with (L)-ascorbate, and stabilized by TBTA (tris(benzyltriazolylmethyl) amine). Anhydrous DMF (dimethyl formamide) was used as solvent. The reaction took place at 45° C during 24 hours.

The purification of this product (molecule 7) was rather challenging and required several steps. The crude product first underwent several washings with brine and an aqueous KCN solution. Next, it was purified by flash chromatography on silica gel. The final level of purity was achieved through dialysis against methanol.

The acid-mediated cleavage of the t-Boc protective groups yielded the final amphiphilic Janus dendrimer (molecule 8).

These molecules were likewise characterized by  $^1\text{H}$  and  $^{13}\text{C}$  NMR, MS, FTIR and EA. The main result that allowed to confirm the correct synthesis of the dendrimer was the appearance in the  $^1\text{H}$  NMR spectrum of the peak corresponding to the proton of the triazole ring, at 7.74 ppm in the spectrum corresponding to molecule 7 and at 8.10 ppm in the spectrum obtained for molecule 8.

The monodispersity of the lipophilic dendron and the Janus dendrimer was confirmed by gel permeation chromatography (GPC). Dispersity values ( $\text{Đ}$ ) obtained were of 1.04 for the lipophilic dendron (molecule 5) and 1.05 for the Janus dendrimer (molecule 8).

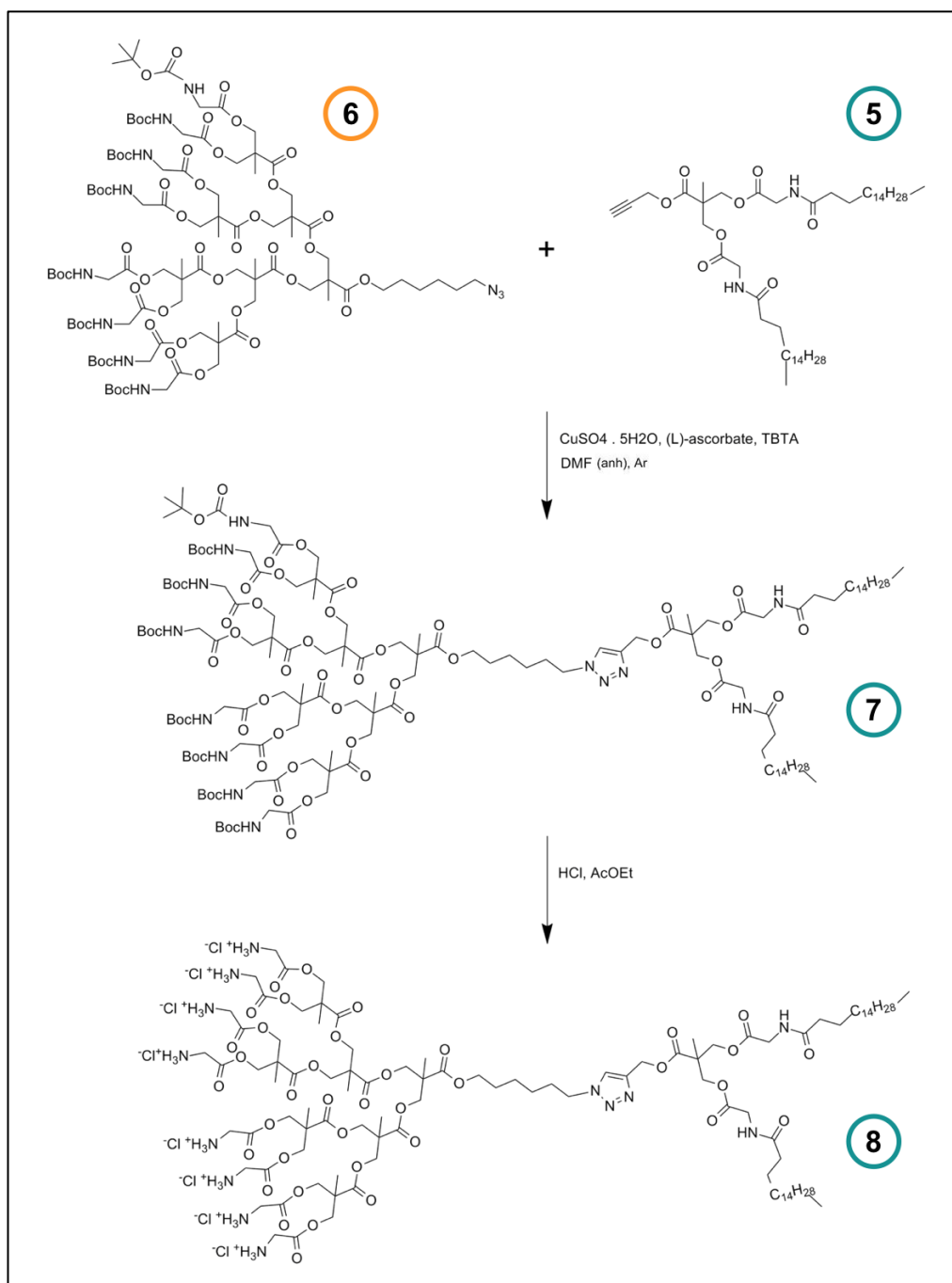


**Figure 10:** Synthesis scheme of reactions leading to the Janus dendrimer (molecule 8).

### 5.3 - Formation of dendritic aggregates and drug encapsulation

The property of self-assembling in aqueous solution of amphiphilic Janus dendrimers was exploited to create structures that could function as drug carriers. These, in turn, were used to encapsulate three different drugs: camptothecin (CPT), tiratricol (TRIAC) and iopanoic acid (IA).

As a first step, aggregates were created using the oil-in-water technique. In this technique, an emulsion is formed composed by a volatile organic solvent in which the dendrimer is dissolved (in this case, dichloromethane) and water. Constant stirring allows the dendrimer to slowly diffuse into the water, forming aggregates as concentration increases due to its amphiphilic properties. The organic solvent evaporates over time, finally leaving an aqueous solution where dendritic aggregates are suspended. These aggregates have a lipophilic core and a hydrophilic shell (exterior), a characteristic that makes them appropriate for transporting hydrophobic substances in a physiological medium.

In order to encapsulate the pharmacological compounds within the nanocarriers, the solvent diffusion technique was used. It consists on adding a solution of the drug in DMSO to the aqueous solution containing the dendritic aggregates and stirring during a sufficient amount of time for the drug to reach the lipophilic core of the carriers (approximately twelve hours). DMSO is then removed by dialysis. The drug that is not encapsulated precipitates in water and is removed by filtration.

It was estimated that the drug/dendrimer proportion of the resulting conjugates would be lower for camptothecin than for tiratricol and iopanoic acid, given the more rigid structure of this drug. For this reason, the feeding ratio used for camptothecin was 0.1/1 ( $\text{weight}_{\text{drug}}/\text{weight}_{\text{dendrimer}}$ ), whereas for tiratricol and iopanoic acid it was 0.5/1 ( $\text{weight}_{\text{drug}}/\text{weight}_{\text{dendrimer}}$ ). Each of the three drug/dendrimer conjugates was prepared by duplicate.

The amount of drug encapsulated in the nanocarriers was determined by fluorescence in the case of CPT and by UV-Vis absorbance in the case of TRIAC and IA. The results are recorded in table 2.

Drug	Conjugate	$\text{weight}_{\text{drug}}/\text{weight}_{\text{dendrimer}}$	$\text{mol}_{\text{drug}}/\text{mol}_{\text{dendrimer}}$	EE (%)
CPT	1	0.08	0.55	76
	2	0.07	0.48	66
TRIAC	3	0.34	1.38	68
	4	0.36	1.48	73
IA	5	0.31	1.39	63
	6	0.33	1.47	67

**Table 2:** Drug/dendrimer weight-to-weight ratio, molar ratio and encapsulation efficiency (EE: percentage of drug mass encapsulated with respect to initial drug mass) of the different conjugates.

The results of camptothecin encapsulation in the new dendrimer, composed by a hydrophilic bis-MPA dendron and a lipophilic bis-GMPA dendron, surpass those observed in the precedent research<sup>[13]</sup>. Janus dendrimers composed of hydrophilic and lipophilic dendrons

based on bis-MPA had yielded camptothecin encapsulation efficiencies of up to 14%. The ones composed by hydrophilic bis-GMPA dendrons and lipophilic bis-MPA dendrons improved camptothecin encapsulation efficiencies up to a maximum of 61%. The new dendrimer shows the ability to encapsulate an amount of camptothecin much superior to the bis-MPA/bis-MPA dendrimers, and slightly higher than the bis-GMPA/bis-MPA dendrimers.

With regard to tiratricol and iopanoic acid, encapsulation in Janus dendrimers based on bis-MPA or bis-GMPA dendrons had not been attempted. The new dendrimer also presents a high efficiency in encapsulating these compounds.

The good results obtained for this dendrimer further confirm that inclusion of a glycine moiety can improve drug encapsulation, arguably because it introduces the possibility of the formation of hydrogen bonds and other interactions between the drug and the carrier. Dendrimers composed of dendrons of different generations should also be studied. However, it is to be noted that the dendrimers that had yielded the best encapsulation efficiencies in the past were composed of lipophilic dendrons of the lowest generation (2 terminal aliphatic chains) and hydrophilic dendrons of eight amino-terminal groups, a structure similar to that of the dendrimer described in this work.

#### 5.4 - Study of the size and morphology of the nanoaggregates

The aggregates, both empty and encapsulating the three different drugs, were characterized by transmission electron microscopy (TEM) and dynamic light scattering (DLS).

TEM imaging was employed to determine the morphology of the nanoaggregates. In this technique a beam of electrons is transmitted through a material; the differential behavior of electrons depending on the characteristics of said material allows to obtain an image.

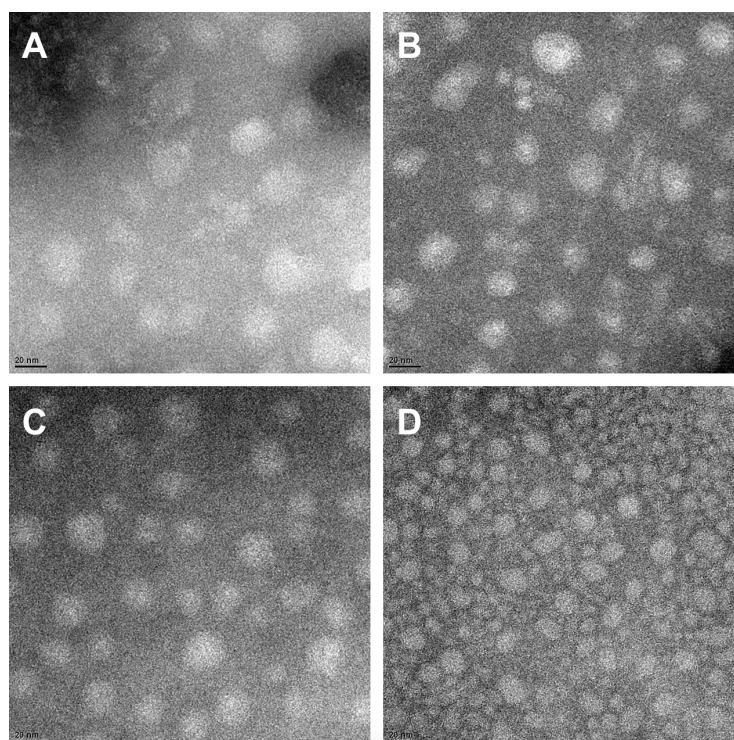


**Figure 11:** Images of the empty aggregates (A), the CPT-loaded aggregates (B), the TRIAC-loaded aggregates (C) and the IA-loaded aggregates (D) obtained by TEM. Scale = 20 nm.

As the bright field operation mode was used, the contrast of the images depends on the thickness, density or atomic number of the sample: the higher these are in a certain region, the darker this region will appear. Thus, the areas of the grid that have been stained with phosphotungstic acid appear dark in the images, due to the presence of tungstene, a heavy metal. Areas where nanoaggregates are adsorbed will be devoid of the phosphotungstic acid, and will appear bright. It is important to note that the images obtained are therefore not a direct representation of the aggregates.

In all cases the aggregation of the dendrimer appears to have resulted in spherical micelles. This morphology remains unchanged as a result of drug encapsulation. It can also be observed that while the other aggregates (A, B and C in figure 11) appear to be isolated, the micelles containing iopanoic acid (D in figure 11) seem to interact forming a reticular pattern.

The size of the particles was measured both on the TEM images and by DLS.

DLS provided a value of the hydrodynamic diameter (diameter of a hypothetical hard sphere that presents the same diffusional behavior as that of the dynamic hydrated or solvated particle measured). The results obtained have been processed using two different mathematical approaches: number and intensity. The former is more sensitive to small particles, while the latter allows to detect bigger aggregations.

The width values measured on TEM images and the DLS number and DLS intensity average data are presented in table 3.

Aggregate	TEM width	DLS (number) D <sub>H</sub>	DLS (intensity) D <sub>H</sub>
Dendrimer	24 ± 4 nm	13 ± 2 nm	352 ± 160 nm
CPT/dendrimer	23 ± 5 nm	696 ± 84 nm	681 ± 81 nm & 1869 ± 187 nm
TRIAC/dendrimer	24 ± 4 nm	20 ± 5 nm	204 ± 131 nm
IA/dendrimer	19 ± 3 nm	15 ± 3 nm	143 ± 34 nm & 631 ± 162 nm

**Table 3:** Sizes of the empty or drug-loaded aggregates obtained by TEM or DLS (mean ± standard deviation).

The DLS number values are consistent with those extracted from the TEM images, except for the ones obtained for the camptothecin/dendrimer conjugate. However, this can be explained by the fact that camptothecin is a fluorescent compound, so it interacts with light making DLS measurements not reliable. These results (TEM and DLS number) correspond to the sizes of the isolated micelles. Particle size does not appear to vary significantly as a result of drug encapsulation, except for a slight shrinking observed in the microscopy images of the iopanoic acid/dendrimer conjugate.

DLS intensity data indicate the presence of bigger aggregates<sup>[21]</sup>. These present a great dispersion in sizes, which translates into high standard deviations. It can therefore be deduced that these sizes correspond to clusters of micelles possibly formed due to non-specific interactions. This effect is more noticeable in the case of iopanoic acid, where a population of aggregates of around 630 nm has been found (not counting the data

corresponding to the CPT/dendrimer conjugate, which are not reliable). This is coherent with the observations made regarding TEM images.

## 5.5 - Isothermal titration calorimetry

Isothermal Titration Calorimetry was used to analyze the thermodynamics of the interactions produced between the dendrimer and the different drugs. For this technique, a solution containing the dendrimer is placed inside the sample cell and a solution containing the ligand (camptothecin, tiratricol or iopanoic acid) is titrated into this cell until saturation of the dendrimer occurs.

The amount of heat released or absorbed as a result of the interactions between both molecules is measured and represented in a thermogram (figure 11, top part). Each peak corresponds to one injection of ligand and is proportional to the amount of heat involved in the formation of the drug-dendrimer complex. The peaks are then integrated with respect to time and normalized for concentration to generate a titration curve representing kcal/mol vs ligand/sample molar ratio (figure 11, bottom part).

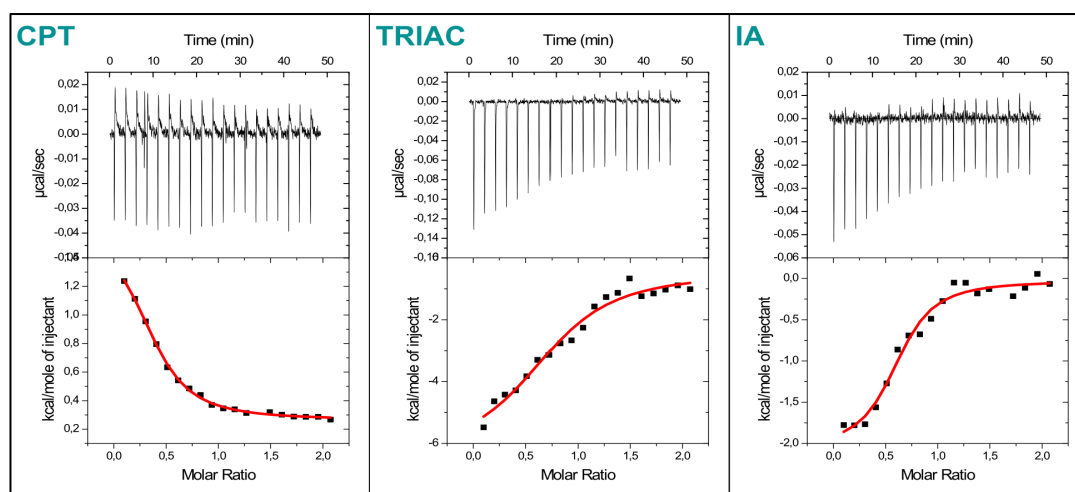


**Figure 12:** Thermograms and titrations curves obtained by ITC, describing interaction between each of the drugs and the dendrimer.

Binding affinity ( $K_a$ ), enthalpy changes ( $\Delta H$ ), and binding stoichiometry ( $N$ ) were calculated by fitting the titration curve to a binding model considering one set of ligand binding sites. The results are recorded in table 4.

	CPT/dendrimer	TRIAC/dendrimer	IA/dendrimer
$K_a$ ( $M^{-1}$ )	850000 $\pm$ 90000	550000 $\pm$ 30000	1800000 $\pm$ 70000
$\Delta H$ (kcal/mol)	1360 $\pm$ 60	- 6000 $\pm$ 1000	- 2000 $\pm$ 200
$N$ (mol drug/mol dendrimer)	0.38 $\pm$ 0.01	0.78 $\pm$ 0.06	0.64 $\pm$ 0.03

**Table 4:** Thermodynamic parameters calculated for each of the drug/dendrimer complexes ( $\pm$  standard deviation).

Iopanoic acid exhibits a higher affinity for the dendrimer in comparison with camptothecin and tiratricol. This could explain the smaller size of the micelles containing iopanoic acid and the higher aggregation described between them (figure 11D and table 3).

The  $\Delta H$  value is positive for the CPT/dendrimer interaction and negative for the TRIAC/dendrimer interaction and the IA/dendrimer interaction. This could mean that in the case of camptothecin, hydrophobic interactions contribute more to the formation of the complex than specific interactions, while the opposite happens with the other two compounds. In absolute values, the greatest enthalpy change has been observed for the formation of the TRIAC/dendrimer complex.

The highest binding stoichiometry has been found for the TRIAC/dendrimer complex, 0.78, followed by the IA/dendrimer complex, 0.64. The CPT/dendrimer complex presents the lowest binding stoichiometry, 0.38. There is a qualitative correlation between this and the drug/dendrimer molar ratios calculated for the encapsulated drugs (table 2), which were also lowest in the case of the carriers loaded with camptothecin. Binding stoichiometries and molar ratios, however, do not match quantitatively; this could be explained by the different conditions of time and concentration in which the processes of the titration and the encapsulation were carried out.

## 5.6 - Cell viability and drug inhibition

The purpose of encapsulating camptothecin, tiratricol and iopanoic acid within the nanocarrier was to enhance the activity of these drugs against the Hepatitis C virus. With respect to camptothecin, the aim was also to lower its cytotoxicity. Besides from assessing whether these objectives had been achieved, it was necessary to ensure that the dendrimer did not affect cell viability. The procedures followed are described in section 4.8 (pages 12-13). In both assays, the effects of the encapsulated drug were compared to those of the free drug and to those of the free dendrimer. A negative control was used as a reference.

### Camptothecin

Figure 13 compares the effects of free and encapsulated camptothecin on cell viability and viral replication.

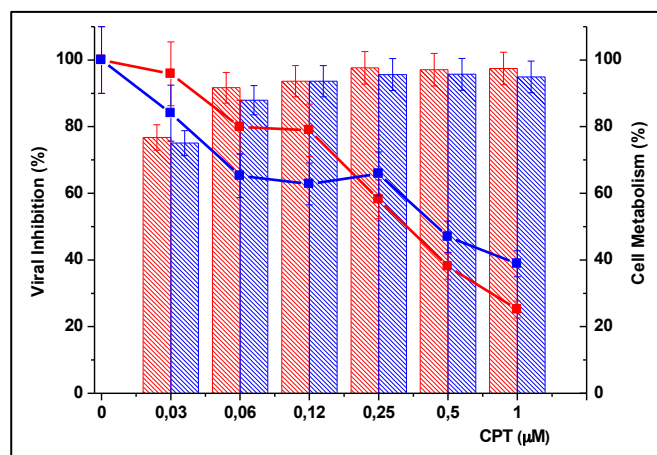


**Figure 13:** Viral replication (bars) and cell viability (lines) against concentration of encapsulated camptothecin (red) and free camptothecin (blue). The left vertical axis represents viral inhibition (%), the left vertical axis represents cell metabolism (%) and the horizontal axis represents CPT concentration (µM). Error bars are shown in the graph.



The IC50 value could not be calculated due to the high inhibition values observed in this assay (above 70% and reaching 100%). Previous studies published in our group carried out with the same drug concentrations reported an IC50 value of 0.3  $\mu\text{M}$  for free camptothecin<sup>[11]</sup>. Concerning cell viability, the CC50 value of free camptothecin estimated as a result of this work coincides with the value reported in these previous studies, 0.6  $\mu\text{M}$ . It can therefore be inferred that the higher levels of viral inhibition observed are not the result of a lower cell viability.

The antiviral activity of the encapsulated drug is similar to that of the free drug, albeit slightly higher. At low CPT concentrations (0.03 - 0.13  $\mu\text{M}$ ), viability remains higher for cells treated with the encapsulated drug. This suggests that using the new dendrimer as a drug carrier could broaden the therapeutic window of camptothecin, allowing to obtain results of viral inhibition similar to those obtained with the free drug but with a lower cytotoxicity. These results must nonetheless be confirmed, especially since they differ from what was observed in previous studies.

#### Tiratricol and iopanoic acid

HCV replication assays did not yield representative results, since a direct correlation between viral inhibition and drug concentration (either free or encapsulated) could not be determined. However, encapsulation in the dendritic aggregates seemed to increase the antiviral activity of these drugs. Again, the free form of these compounds showed a higher activity in this assay compared to data observed in the previous studies<sup>[7]</sup>. The IC50 values estimated as a result of this assay were of 7.25  $\mu\text{M}$  for tiratricol and of 7.50  $\mu\text{M}$  for iopanoic acid, whereas the reported IC50 values were of around 25  $\mu\text{M}$  for tiratricol and of >120  $\mu\text{M}$  for iopanoic acid. With respect to cell viability, the assays showed that no cytotoxicity was derived from these drugs or the corresponding drug/dendrimer conjugates.

As a summary, IC50 and CC50 values estimated for the free compounds and the encapsulated compounds are represented in table 5. Cells incubated with the free dendrimer at the same concentrations present in the assays carried out with encapsulated drugs did not exhibit any viral inhibition or viability reduction (data not shown).

Compound	IC50 ( $\mu\text{M}$ )		CC50 ( $\mu\text{M}$ )	
	Free drug	Encapsulated drug	Free drug	Encapsulated drug
<b>CPT</b>	< 0.03	< 0.03	0.60	0.25
<b>TRIAC</b>	7.25	1.25	> 120	> 120
<b>IA</b>	7.50	5.00	> 120	> 120

**Table 5:** IC50 and CC50 of the free and encapsulated compounds determined in this experiment. Errors in all cases are comprised within an interval of 5-10%.

Camptothecin, tiratricol and iopanoic acid all showed unusually high antiviral activities in this experiment. This suggests that there could be a problem related to the replicon system of the Huh 5-2 cells: for instance, the number of replicon copies per cell could have decreased. Hence, it is necessary to repeat the experiment after selecting and increasing the number of replicon copies in the cell line.

This can only be considered a preliminary study. As a general rule, due to the great number of variables that condition an experiment with living cells, it is important to repeat these assays in several different occasions in order to obtain reproducible results.

## 6 - CONCLUSIONS / CONCLUSIONES

The following **conclusions** can be drawn from the results obtained throughout this project:

- A new lipophilic dendron based on bis-GMPA has been synthesized. This building block has led to the synthesis of an amphiphilic Janus dendrimer composed by the bis-GMPA lipophilic dendron and a bis-MPA hydrophilic dendron.
- The new dendrimer has been proved to form micellar aggregates in water. These aggregates are able to encapsulate camptothecin, tiratricol and iopanoic acid with a high efficiency, improving the results obtained with Janus dendrimers in previous studies.
- Encapsulation of the different drugs does not significantly change the properties of size and morphology of the dendritic aggregates.
- Isothermal titration calorimetry has allowed to describe the interaction between the different drugs and the dendrimer. The thermodynamic parameters of the interaction processes have been determined.
- The dendrimer does not seem to affect cell viability *in vitro*. Cell viability after incubation with the drug/dendrimer conjugates was also seen to be adequate.
- The anti-HCV activity of the drugs encapsulated in the new nanocarrier could not be appropriately determined.

Se pueden extraer las siguientes **conclusiones** de los resultados obtenidos a lo largo de este proyecto:

- Se ha sintetizado un nuevo dendrón lipófilo basado en bis-GMPA. Este bloque básico ha permitido la síntesis de un dendrímero Jano anfífilo compuesto por el dendrón lipófilo de bis-GMPA y un dendrón hidrófilo de bis-MPA.
- Se ha comprobado la capacidad de formar micelas en agua del nuevo dendrímero. Estos agregados son capaces de encapsular camptotecina, tiratricol y ácido iopanoico con una alta eficiencia, mejorando los resultados obtenidos con dendrímeros Jano en estudios anteriores.
- La encapsulación de los diferentes fármacos no cambia de manera significativa las propiedades de tamaño y morfología de los agregados dendríticos.
- Se ha podido describir la interacción entre los distintos fármacos y el dendrímero por calorimetría isotérmica de titulación. Los parámetros termodinámicos de los procesos de interacción se han determinado.
- El dendrímero no parece afectar a la viabilidad celular *in vitro*. Se ha observado asimismo que la viabilidad celular tras la incubación con los complejos fármaco/dendrimer es adecuada.
- La actividad anti-VHC de los fármacos enapsulados no pudo ser determinada de manera apropiada.

## 7 - BIBLIOGRAPHY

1. Fabrizi F, Verdesca S, Messa P, Martin P. Hepatitis C Virus Infection Increases the Risk of Developing Chronic Kidney Disease: A Systematic Review and Meta-Analysis. *Digestive Diseases and Sciences*. **2015**;60(12):3801-13.
2. <http://www.who.int/en/> (cited June 26, 2017).
3. Manns MP, Buti M, Gane E, Pawlotsky J-M, Razavi H, Terrault N, et al. Hepatitis C virus infection. *Nature Reviews Disease Primers*. **2017**;3:nrdp20176.
4. Bastos JCS, Padilla MA, Caserta LC, Miotto N, Vigani AG, Arns CW. Hepatitis C virus: Promising discoveries and new treatments. *World Journal of Gastroenterology*. **2016**;22(28):6393.
5. Abián O, Neira JL, Velázquez-Campoy A. Thermodynamics of zinc binding to hepatitis C virus NS3 protease: a folding by binding event. *Proteins*. **2009**;77(3):624-36.
6. Abián O, Vega S, Sancho J, Velázquez-Campoy A. Allosteric Inhibitors of the NS3 Protease from the Hepatitis C Virus. *PLOS ONE*. **2013**;8(7):e69773.
7. Clavería-Gimeno R, Vega S, Grazú V, de la Fuente JM, Lanás A, Velázquez-Campoy A, Abián O. Rescuing compound bioactivity in a secondary cell-based screening by using  $\gamma$ -cyclodextrin as a molecular carrier. *International Journal of Nanomedicine*. **2015**;10:2249-59.
8. Hsu H-J, Bugno J, Lee S-R, Hong S. Dendrimer-based nanocarriers: a versatile platform for drug delivery. *Wiley Interdisciplinary Reviews. Nanomedicine and Nanobiotechnol.* **2017**;9(1).
9. Caminade A-M, Laurent R, Delavaux-Nicot B, Majoral J-P. «Janus» dendrimers: syntheses and properties. *New Journal of Chemistry*. **2012**;36(2):217-26.
10. Fedeli E, Lancelot A, Serrano JL, Calvo P, Sierra T. Self-assembling amphiphilic Janus dendrimers: mesomorphic properties and aggregation in water. *New Journal of Chemistry*. **2015**;39(3):1960-7.
11. Lancelot A, Clavería-Gimeno R, Velázquez-Campoy A, Abián O, Serrano JL, Sierra T. Nanostructures based on ammonium-terminated amphiphilic Janus dendrimers as camptothecin carriers with antiviral activity. *European Polymer Journal*. **2017**;90:136-49.
12. Carlmark A, Malmström E, Malkoch M. Dendritic architectures based on bis-MPA: functional polymeric scaffolds for application-driven research. *Chemical Society Reviews*. **2013**;42(13):5858-79.

13. Lancelot A. New dendritic derivatives for applications in nanomedicine: drug delivery and gene transfection. **2017**, Universidad de Zaragoza.
14. Movellan J, Urbán P, Moles E, de la Fuente JM, Sierra T, Serrano JL, Fernández-Busquets X. Amphiphilic dendritic derivatives as nanocarriers for the targeted delivery of antimalarial drugs. *Biomaterials*. **2014**;35(27):7940-50.
15. Jiménez-Pardo I, González-Pastor R, Lancelot A, Clavería-Gimeno R, Velázquez-Campoy A, Abián O, Ros MB, Sierra T. Shell Cross-Linked Polymeric Micelles as Camptothecin Nanocarriers for Anti-HCV Therapy. *Macromolecular Bioscience*. **2015**;15(10):1381-91.
16. Pierce MM, Raman CS, Nall BT. Isothermal titration calorimetry of protein-protein interactions. *Methods*. **1999**;19(2):213-21.
17. Lohmann V, Körner F, Koch J, Herian U, Theilmann L, Bartenschlager R. Replication of subgenomic hepatitis C virus RNAs in a hepatoma cell line. *Science*. **1999**;285(5424):110-3.
18. Bartenschlager R. Hepatitis C virus replicons: potential role for drug development. *Nature Reviews Drug Discovery*. **2002**;1(11):911-6.
19. Ashfaq UA, Javed T, Rehman S, Nawaz Z, Riazuddin S. An overview of HCV molecular biology, replication and immune responses. *Virology Journal*. **2011**;8:161.
20. Bartenschlager R. The hepatitis C virus replicon system: From basic research to clinical application. *Journal of Hepatology*. **2005**;43(2):210-6.
21. Hed Y, Zhang Y, Andrén OCJ, Zeng X, Nyström AM, Malkoch M. Side-by-side comparison of dendritic-linear hybrids and their hyperbranched analogs as micellar carriers of chemotherapeutics. *Journal of Polymer Science Part A: Polymer Chemistry*. **2013**;51(19):3992-6.